The EMBO Journal (2009) 28, 3717–3729 | © 2009 European Molecular Biology Organization | All Rights Reserved 0261-4189/09
www.embojournal.org

THE EMBO JOURNAL

Involvement of NMDAR2A tyrosine phosphorylation in depression-related behaviour

Sachiko Taniguchi[1,10], Takanobu Nakazawa[1,10,*], Asami Tanimura[2,10], Yuji Kiyama[3], Tohru Tezuka[1,11], Ayako M Watabe[3], Norikazu Katayama[3], Kazumasa Yokoyama[1], Takeshi Inoue[1], Hiroko Izumi-Nakaseko[3,12], Shigeru Kakuta[4], Katsuko Sudo[4,13], Yoichiro Iwakura[4], Hisashi Umemori[5], Takafumi Inoue[6], Niall P Murphy[7], Kouichi Hashimoto[2,8], Masanobu Kano[2], Toshiya Manabe[3,8] and Tadashi Yamamoto[1,9]

[1]Division of Oncology, Institute of Medical Science, University of Tokyo, Tokyo, Japan, [2]Department of Neurophysiology, Graduate School of Medicine, University of Tokyo, Tokyo, Japan, [3]Division of Neuronal Network, Institute of Medical Science, University of Tokyo, Tokyo, Japan, [4]Center for Experimental Medicine and Systems Biology, Institute of Medical Science, University of Tokyo, Tokyo, Japan, [5]Molecular & Behavioral Neuroscience Institute and Department of Biological Chemistry, University of Michigan Medical School, Ann Arbor, MI, USA, [6]Department of Life Science and Bio-science, Faculty of Science and Engineering, Waseda University, Tokyo, Japan, [7]Hatos Center for Neuropharmacology, Department of Psychiatry and Biobehavioral Sciences, UCLA Semel Institute for Neuroscience and Human Behavior, Los Angeles, CA, USA, [8]Core Research for Evolutional Science and Technology (CREST), Japan Science and Technology Agency (JST), Kawaguchi, Japan and [9]Laboratory of Molecular Biology, NCI, National Institutes of Health, Bethesda, MD, USA

Major depressive and bipolar disorders are serious illnesses that affect millions of people. Growing evidence implicates glutamate signalling in depression, though the molecular mechanism by which glutamate signalling regulates depression-related behaviour remains unknown. In this study, we provide evidence suggesting that tyrosine phosphorylation of the NMDA receptor, an ionotropic glutamate receptor, contributes to depression-related behaviour. The NR2A subunit of the NMDA receptor is tyrosine-phosphorylated, with Tyr 1325 as its one of the major phosphorylation site. We have generated mice expressing mutant NR2A with a Tyr-1325-Phe mutation to prevent the phosphorylation of this site *in vivo*. The homozygous knock-in mice show antidepressant-like behaviour in the tail suspension test and in the forced swim test. In the striatum of the knock-in mice, DARPP-32 phosphorylation at Thr 34, which is important for the regulation of depression-related behaviour, is increased. We also show that the Tyr 1325 phosphorylation site is required for Src-induced potentiation of the NMDA receptor channel in the striatum. These data argue that Tyr 1325 phosphorylation regulates NMDA receptor channel properties and the NMDA receptor-mediated downstream signalling to modulate depression-related behaviour.

The EMBO Journal (2009) **28,** 3717–3729. doi:10.1038/emboj.2009.300; Published online 15 October 2009
Subject Categories: signal transduction; neuroscience
Keywords: DARPP-32; depression-related behaviour; NMDA receptor; Src; tyrosine phosphorylation

Introduction

Depression is a severe neuropsychiatric disorder that features a combination of depressed mood feelings, such as sadness, hopelessness, helplessness, and/or worthlessness. The lifetime risk for major depressive disorder and bipolar disorders in the United States is ~10% as defined by DSM IV. Challenges of establishing the molecular mechanisms underlying depression and of discovering improved therapeutic agents to treat depression are important (Zarate *et al*, 2006). The serotonergic, noradrenergic, and dopaminergic systems have received great attention in studies related to mood disorders (Sanacora *et al*, 2008). In addition to these systems, the glutamatergic pathway, a major mediator of excitatory synaptic transmission in the mammalian brain, has been the focus of the pathophysiological study of mood disorders (Orrego and Villanueva, 1993; Sanacora *et al*, 2008). The agents that act on the glutamatergic pathway are promising candidates for the treatment of mood disorders (Sanacora *et al*, 2008). In rodents, treatment with competitive *N*-methyl-D-aspartate (NMDA) subtype of ionotropic glutamate receptor (NMDA receptor) antagonists produced antidepressant-like effects in several behavioural tasks, including the forced swim test (Trullas and Skolnick, 1990). Genetic evidence for the involvement of the glutamatergic pathway in emotional regulation has been obtained by analysing mice with genetically engineered NMDA receptor genes (Mohn *et al*, 1999; Miyamoto *et al*, 2001; Boyce-Rustay and Holmes, 2006). Although these previous findings suggest the involvement of the NMDA receptor in depression-related behaviour, the underlying molecular mechanism remains unclear.

A number of neuronal functions such as synaptic plasticity are rapidly and reversibly regulated in response to external factors. Phosphorylation reaction is a key process in the regulation of various neuronal functions because it can rapidly and reversibly change the function of cellular proteins, including NMDA receptor subunits. The NMDA receptor is crucial for development, synaptic plasticity, and

*Corresponding author. Division of Oncology, Institute of Medical Science, University of Tokyo, 4-6-1 Shirokanedai, Minato-ku, Tokyo 108-8639, Japan. Tel.: +81 3 5449 5305; Fax: +81 3 5449 5413; E-mail: takanobunakazawa-tky@umin.ac.jp
[10]These authors contributed equally to this work
[11]Present address: Division of Genetics, Institute of Medical Science, University of Tokyo, Tokyo 108-8639, Japan
[12]Present address: Department of Pharmacology, School of Medicine, Faculty of Medicine, Toho University, Tokyo, 143-8540, Japan
[13]Present address: Animal Research Center, Tokyo Medical University, Tokyo, 160-8402, Japan

Received: 7 April 2009; accepted: 9 September 2009; published online: 15 October 2009

neuronal excitotoxicity (Choi, 1988; McDonald and Johnston, 1990; Collingridge and Bliss, 1995). The NMDA receptor is composed of NR1 (GluRζ) and NR2 (GluRε) subunits: the NR1 subunit is essential for the function of NMDAR channels, whereas NR2 subunits (NR2A (GluRε1), NR2B (GluRε2), NR2C (GluRε3), and NR2D (GluRε4)) determine the characteristics of NMDAR channels by forming different heteromeric configurations with the NR1 subunit (Kutsuwada *et al*, 1992; Monyer *et al*, 1992; Ishii *et al*, 1993; Cull-Candy *et al*, 2001). The NR1 and NR2 subunits contain phosphorylation sites that seem to have key roles in regulating NMDA receptor localization and channel activity, as well as downstream signalling via NMDA receptor-associated proteins (Kornau *et al*, 1997; Husi *et al*, 2000; Scannevin and Huganir, 2000; Nakazawa *et al*, 2001, 2006; Sheng and Kim, 2002; Salter and Kalia, 2004; Chen and Roche, 2007; Okabe, 2007). Biochemical studies have found that non-receptor tyrosine kinases, Src and Fyn, phosphorylate NR2A and NR2B (Yang and Leonard, 2001; Salter and Kalia, 2004; Nakazawa *et al*, 2001, 2006; Chen and Roche, 2007). NR2A and NR2B contain several tyrosine phosphorylation sites (Yang and Leonard, 2001; Salter and Kalia, 2004; Nakazawa *et al*, 2001, 2006; Chen and Roche, 2007). Tyr 1472 phosphorylation, the principal tyrosine phosphorylation event on NR2B, regulates amygdaloid synaptic plasticity, and fear-related learning (Nakazawa *et al*, 2006), however, the role of Tyr 1325 phosphorylation on NR2A remains unknown.

In this study, we investigated the role of Tyr 1325 phosphorylation on NR2A with knock-in mice in which Tyr 1325 of NR2A is mutated to phenylalanine. Using biochemical, genetic, and electrophysiological approaches with the knock-in mice, we provide evidence of a critical involvement of Tyr 1325 phosphorylation in depression-related behaviour.

Results

Tyr 1325 as one of the principal Src family kinase-mediated phosphorylation sites

The NR2A subunit of the NMDA receptor contains 25 tyrosine residues in the intracellular C-terminal region. To determine the Src family kinase-mediated NR2A phosphorylation sites, we constructed GST fusion proteins containing truncated segments of the NR2A C-terminal region (termed GST–C1, GST–C2, and GST–C3) (Figure 1A). These fusion proteins were phosphorylated by baculovirally expressed Fyn in the presence of [γ-^{32}P]ATP. The phosphorylated proteins were subjected to tryptic phosphopeptide mapping. As shown in Figure 1B, highly phosphorylated peptides P1–P7 were generated from the phosphorylated GST–fusion proteins. To identify the tyrosine residue in most prominently phosphorylated P7 peptide, we constructed Y1325F (conversion of Tyr 1325 to Phe 1325)–GST–C2 protein by site-directed mutagenesis, and performed the *in vitro* phosphorylation assay as above. Conversion of Tyr 1325 to Phe 1325 resulted in generation of a tryptic phosphopeptide map that lacked phosphopeptide P7, suggesting that Tyr 1325 was most prominently phosphorylated by Fyn *in vitro* (Figure 1B). Similarly, phosphorylated tyrosines in other phosphopeptides were examined by introducing YF mutations in the GST–C1 and GST–C2 proteins. We found that Tyr 943, Tyr 1105, Tyr 1118, Tyr 1187, Tyr 1246, and Tyr 1267 were also phosphorylated *in vitro* (data not shown). As Tyr 1325 was most strongly phosphorylated *in vitro*, we examined whether Tyr 1325 was phosphorylated in cells (Figure 1C). HEK 293T cells were transfected with expression plasmids encoding wild-type or Y1325F mutant forms of the NR2A subunit along with a plasmid encoding Src YF, a constitutively active

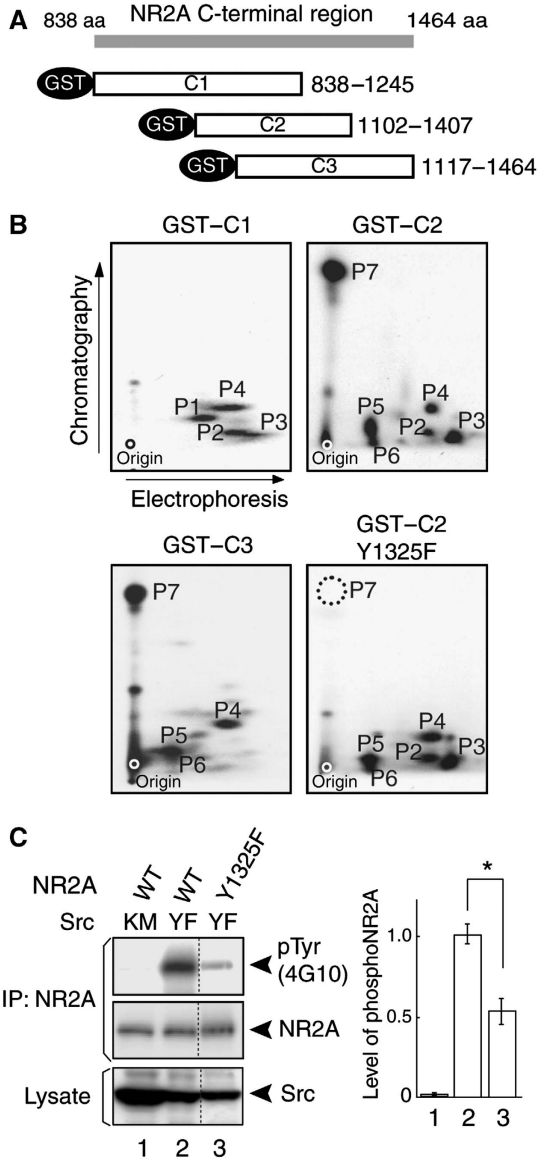

Figure 1 Identification of Tyr 1325 as one of the principal Src family kinase-mediated phosphorylation sites of the NR2A subunit. (**A**) Schematic diagram of GST fusion proteins containing the intracellular C-terminal region of the NR2A subunit. (**B**) Two-dimensional tryptic phosphopeptide maps of GST–C1, GST–C2, GST–C2–Y1325F, and GST–C3. The dot in each map shows the origin of electrophoresis. Note that P7 (Tyr 1325) was most prominently phosphorylated *in vitro*. (**C**) Identification of Tyr 1325 as one of the principal phosphorylation sites in HEK 293T cells. HEK293T cells were transfected with combinations of expression plasmids for the NR2A subunit, NR2A Y1325F mutants, and active Src (SrcYF) or inactive Src (SrcKM). NR2A immunoprecipitates from cell lysates were subjected to immunoblotting using the anti-pY antibody (4G10) (top), followed by a re-blot using the anti-NR2A antibody (middle). The expression levels of Src were confirmed by immunoblotting (bottom). *$P<0.001$, $n=4$, Student's *t*-test. Note that all lanes are from the same gel, but lanes originally present between lanes 2 and 3 have been omitted for brevity.

form of Src. Immunoblotting of NR2A immunoprecipitates with the 4G10 anti-phosphotyrosine antibody revealed that Y1325F mutation significantly decreased the tyrosine phosphorylation level of the NR2A subunits ($n=4$; $^*P<0.001$, Student's t test; Figure 1C). The data suggest that Tyr 1325 was one of the principal Src-mediated phosphorylation sites in HEK 293T cells as well as *in vitro*.

Point mutation of Tyr 1325 on NR2A blocks Src-mediated potentiation of NMDA receptor currents

We next addressed the biological significance of Tyr 1325 phosphorylation. As NR2A phosphorylation by Src is suggested to potentiate NMDA receptor currents (Wang and Salter, 1994; Kohr and Seeburg, 1996; Yu *et al*, 1997), we examined the effect of null phosphorylation at Tyr 1325 by introducing Y1325F mutation in NR2A. Heteromeric NMDA receptor channels consisting of NR1 and wild-type NR2A or Y1325F mutant (Y1325F–NR2A) were transiently expressed in HEK 293T cells and NMDA-evoked whole cell currents were recorded. The current mediated by the NMDA receptor channel with wild-type NR2A subunits was potentiated by the application of the Src protein through patch pipette (Figure 2A). In contrast, the current mediated by the NMDA receptor channel with Y1325F–NR2A subunits was minimally potentiated by the Src protein (Figure 2A). To confirm the lack of Src-dependent NMDA receptor potentiation by Y1325F mutation, we examined the effect on Ca^{2+} influx. HEK293T cells were transfected with expression plasmids encoding NR1 and wild-type (WT) or Y1325F mutant forms of NR2A together with or without active Src. After that the cells were loaded with fura2/AM and stimulated using NMDA. As shown in Figure 2B, a marked increase of Ca^{2+} concentration was observed in cells expressing NR1/WT–NR2A and active Src after NMDA stimulation, as compared with that in cells expressing NR1/WT–NR2A alone. In contrast, the level of increase in Ca^{2+} in cells expressing NR1/Y1325F–NR2A and active Src was virtually identical to that in cells expressing NR1/Y1325F–NR2A alone (Figure 2B). These data suggest that Tyr 1325 phosphorylation is required for Src-mediated potentiation of NMDA receptor currents to modulate Ca^{2+} signalling downstream of NMDA receptors.

Generation of NR2A Y1325F knock-in mice

To examine the physiological role of NR2A Tyr 1325 phosphorylation, we generated mutant mice in which Tyr 1325 was substituted with Phe 1325 by a knock-in technique (Figure 3A). The success of these procedures was confirmed by Southern blot and PCR analysis (data not shown). We confirmed the absence of Tyr 1325 phosphorylation in homozygous knock-in mice (YF/YF mice) by immunoblot analysis using the anti-pY1325 antibody that specifically recognizes NR2A phosphorylated at Tyr 1325 (Figure 3B

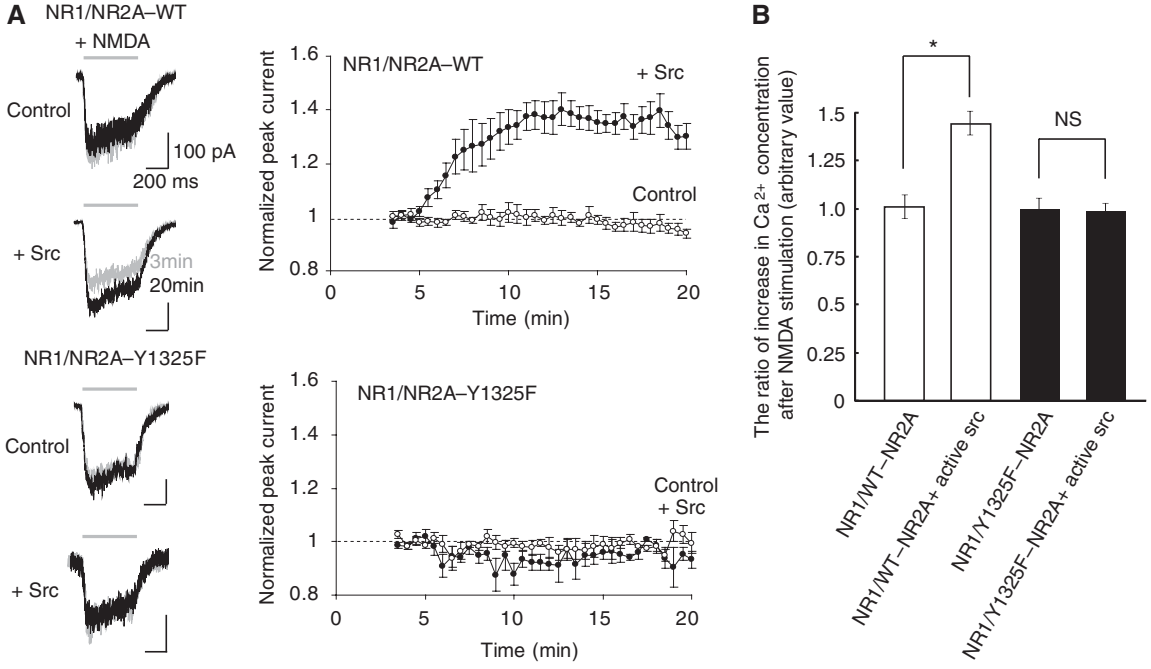

Figure 2 Point mutation at Tyr 1325 on the NR2A subunit blocks Src-mediated potentiation of recombinant NMDA receptor currents in HEK 293T cells. (**A**) Application of Src differentially potentiated NMDA-activated currents mediated by recombinant NR1–wild-type (WT) NR2A channels (upper), but not those mediated by recombinant NR1–Y1325F NR2A channels (lower). Peak currents evoked by NMDA applications (100 μM NMDA and 10 μM glycine: 0.5 s) at 30-s intervals were normalized to the first responses at 3 min after establishing whole-cell configuration (time: 0 min; holding potential: −60 mV). Src (30 U/ml) was added to the internal pipette solution. WT NR2A (control), $n=5$; WT NR2A (+Src), $n=6$; Y1325F NR2A (control), $n=4$; Y1325F NR2A (+Src), $n=5$. Representative averaged whole-cell currents evoked at −60 mV by the NMDA application are shown in the left panel and the traces recorded at 3 min (grey) and 20 min (black) are superimposed. Scale bars: 0.2 s; 100 pA. (**B**) Src-dependent increment of free calcium levels in cells expressing NR1/wild-type NR2A, but not NR1/Y1325F–NR2A channel. Intracellular free calcium levels, before and after NMDA stimulation in fura-2/AM-loaded cells, were monitored by spectrofluorometry. Increase in the ratio of the fluorescence intensities at excitation wavelengths of 340 nm (Fex340) and 380 nm (Fex380) after NMDA stimulation are shown ($n=4$, $^*P<0.05$, Student's t-test). NS: not significant.

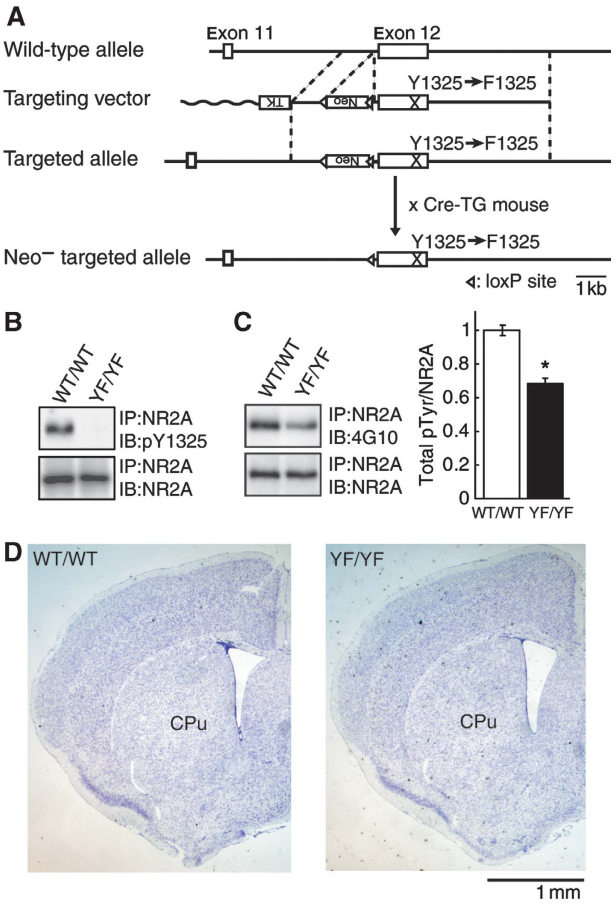

Figure 3 Generation of mice with a mutation of Tyr 1325 phosphorylation site on NR2A. (**A**) Schematic representations of the structures of wild-type, targeting vector, and targeted and Neo-targeted NR2A alleles. *TK*, thymidine kinase gene; *neo*, neomycin resistance gene. (**B**) Absence of Tyr 1325 phosphorylation in homozygous YF/YF mice. Equal amounts of brain lysates from WT/WT and YF/YF mice were probed with the anti-pY1325 antibody followed by a re-blot using the anti-NR2A antibody. (**C**) NR2A tyrosine-phosphorylation in YF/YF mice. Equal amounts of NR2A immunoprecipitates from striatal lysates of WT/WT and YF/YF mice were probed with the anti-phosphotyrosine (4G10) antibody followed by a re-blot with the anti-NR2A antibody. A representative blot is shown on the left ($^*P<0.01$, $n=3$, Student's *t*-test). (**D**) Nissl-stained coronal sections of central nervous system structures including striatum from WT/WT and YF/YF mice. Cpu: Caudata-putamen.

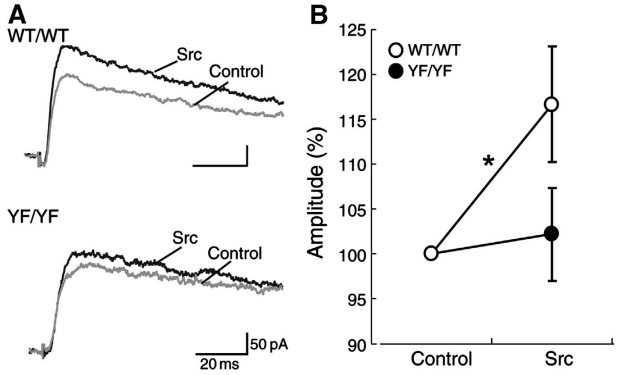

Figure 4 Src-induced potentiation of NMDA receptor-mediated EPSCs is abolished in medium spiny neurons in acute striatal slices from YF/YF mice. (**A**) Examples of NMDA receptor-mediated EPSCs. (**B**) Src-dependent change in the peak amplitude of NMDA receptor-mediated EPSCs in medium spiny neurons from WT/WT and YF/YF mice. WT/WT, $n=15$; YF/YF, $n=11$; $^*P=0.036$, paired *t*-test.

and Supplementary Figure 1). The expression level of NR2A in YF/YF mice was virtually identical to that in wild-type littermates (WT/WT mice) (Figure 3B). In YF/YF mice, the level of NR2A tyrosine phosphorylation was significantly reduced as compared with that in WT/WT mice ($n=3$; $^*P<0.001$, Student's *t* test; Figure 3C), indicating that Tyr 1325 was one the major phosphorylation sites *in vivo* as well as *in vitro* (Figure 1). YF/YF mice were born according to Mendelian genetics and appeared healthy (data not shown). Histological analysis with Nissl-stained coronal sections of central nervous system structures from YF/YF mice did not show any gross abnormalities in cytoarchitecture (Figure 3D). These findings suggest that Tyr 1325 phosphorylation may be relevant to the NMDAR function in mature brain.

Impaired Src-induced potentiation of NMDA receptor-mediated excitatory postsynaptic currents in medium spiny neurons in acute slices from YF/YF mice

To examine the effect of Tyr 1325 phosphorylation on NMDA receptor-mediated excitatory postsynaptic currents (EPSCs) *in vivo*, we performed electrophysiological experiments on medium spiny neurons. Two glass micropipettes were placed in the cerebral cortex or in the underlying white matter to stimulate the corticostriatal axons. Stimulus pulses (duration: 0.1 ms; intensity: 0–80 V) were then applied between the pipettes to evoke EPSCs in medium spiny neurons. Application of the Src protein through a patch pipette potentiated the NMDA receptor-mediated EPSCs in WT/WT slices (Figure 4). In contrast, NMDA receptor-mediated EPSCs were not significantly changed by the Src protein in YF/YF slices (Figure 4). These results suggest that Tyr 1325 phosphorylation is required for Src-induced potentiation of the NMDA receptor-mediated EPSCs in medium spiny neurons, which is consistent with findings from recombinantly expressed NMDA receptor in HEK 293T cells (Figure 2).

Antidepressant-like phenotypes in the forced swim test and the tail suspension test in YF/YF mice

We performed a battery of behavioural tests to examine sensory and motor functions as well as cognition and anxiety of YF/YF mice. The tests revealed that YF/YF mice were less immobile than WT/WT mice in the tail suspension test (Figure 5A and B), one of the most widely used models for assessing antidepressant-like activity in mice (Cryan *et al*, 2005). YF/YF mice also showed significantly less immobility than WT/WT mice in the forced swim test (Figure 5C and D), another test for assessing antidepressant-like activity (Petit-Demouliere *et al*, 2005). Given that, the higher the mobility, mice are less depressive (Cryan *et al*, 2005; Petit-Demouliere *et al*, 2005), we postulated that YF/YF mice were less susceptible to depression than WT/WT mice. Alternatively, the reduced immobility of YF/YF mice in these tests might have been caused by the increase in spontaneous activity (Crawley, 2007). To check this possibility, we performed the open field test to measure spontaneous locomotor activity of YF/YF mice (Figure 5E). The results showed that there were

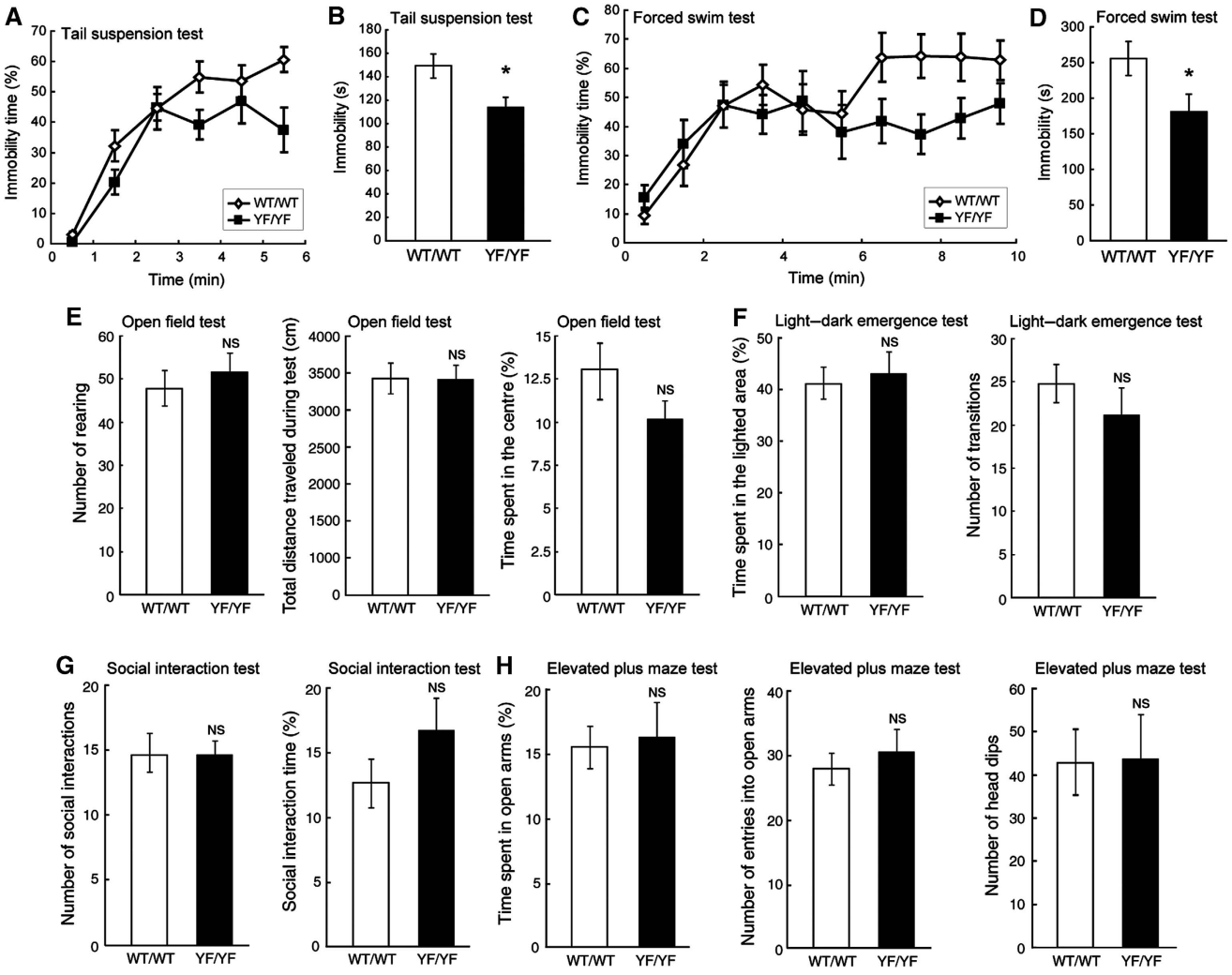

Figure 5 Reduced depression-related behaviour in YF/YF mice. (**A**) Percent immobility of WT/WT and YF/YF mice in the tail suspension test. (**B**) Summary of immobility in the tail suspension test during the last 4 min of the 6-min test session. WT/WT, $n=13$; YF/YF, $n=11$; $F_{(1,22)}=6.00$, $^*P=0.02$, one-way ANOVA. (**C**) Percent immobility of WT/WT and YF/YF mice in the forced swim test. (**D**) Summary of immobility in the forced swim test during the last 7 min of the 10-min test session. WT/WT, $n=12$; YF/YF, $n=12$; $F_{(1,22)}=4.69$, $^*P=0.04$, one-way ANOVA. (**E**) Normal locomotor activity and anxiety-like behaviour of YF/YF mice in the open field test. WT/WT, $n=13$; YF/YF, $n=12$, $P>0.05$, one-way ANOVA. (**F**) Normal anxiety-like behaviour of YF/YF mice in the light–dark emergence test. WT/WT, $n=13$; YF/YF, $n=12$, $P>0.05$, one-way ANOVA. (**G**) Normal behaviour of YF/YF mice in the social interaction test. WT/WT, $n=11$; YF/YF, $n=11$, $P>0.05$, one-way ANOVA. (**H**) Normal anxiety-like behaviour of YF/YF mice in the elevated plus maze test. The time spent on open arms and the number of entries into open arms: WT/WT, $n=13$; YF/YF, $n=12$, $P>0.05$, one-way ANOVA. Number of head dips: WT/WT, $n=10$; YF/YF, $n=10$, $P>0.05$, one-way ANOVA. NS: not significant.

no significant differences between WT/WT and YF/YF mice in the number of rearing (measure the number of beam breaks) (WT/WT, 47.9 ± 4.10, $n=13$; YF/YF, 51.5 ± 4.49, $n=13$; $F_{(1,24)}=0.35$, $P=0.56$, one-way ANOVA) and the total distance travelled during the test (WT/WT, 3435 ± 191 cm, $n=13$; YF/YF, 3400 ± 182 cm, $n=13$; $F_{(1,24)}=0.018$, $P=0.89$, one-way ANOVA), suggesting that spontaneous activity was virtually normal in YF/YF mice. As alteration in fearfulness can also affect the performance in the tests for depression (Crawley, 2007), we also analysed the anxiety-related behaviour. We did not detect any significant abnormality in YF/YF mice in the open field test (the time spent in the centre, WT/WT, $13.0\pm1.78\%$, $n=13$; YF/YF, $10.2\pm1.10\%$, $n=13$; $F_{(1,24)}=1.83$, $P=0.19$, one-way ANOVA; Figure 5E), the light–dark emergence test (the time spent in the lighted area: WT/WT, $40.9\pm3.15\%$, $n=13$; YF/YF, $42.6\pm4.14\%$, $n=13$; $F_{(1,24)}=0.11$, $P=0.74$, one-way ANOVA; the number of transitions: WT/WT, 24.9 ± 2.10, $n=13$; YF/YF, 21.7 ± 2.96, $n=13$; $F_{(1,24)}=0.79$, $P=0.38$, one-way ANOVA; Figure 5F), the social interaction test (the number of social interactions: WT/WT, 14.5 ± 1.7, $n=11$; YF/YF, 14.5 ± 0.8, $n=11$; $F_{(1,20)}=0.002$, $P=0.96$, one-way ANOVA; the social interaction time, WT/WT, $12.7\pm2.06\%$, $n=11$; YF/YF, 16.4 ± 2.66, $n=11$; $F_{(1,20)}=1.18$, $P=0.28$, one-way ANOVA; Figure 5G), and the elevated plus maze test in YF/YF mice (the time on open arms: WT/WT, $15.68\pm1.48\%$, $n=13$; YF/YF, $16.45\pm2.85\%$, $n=13$; $F_{(1,24)}=0.06$, $P=0.81$, one-way ANOVA; the number of entries into open arms: WT/WT, 28.2 ± 2.02, $n=13$; YF/YF, 30.7 ± 2.76, $n=13$; $F_{(1,24)}=0.55$, $P=0.47$, one-way ANOVA; the number of head dips: WT/WT, 42.5 ± 7.69, $n=10$; YF/YF, 43.5 ± 9.89, $n=10$; $F_{(1,18)}=0.006$, $P=0.94$, one-way ANOVA; Figure 5H). In addition, the performance of YF/YF mice in the Morris water maze test, contextual fear conditioning test,

auditory fear conditioning test, acoustic startle response test, pre-pulse inhibition test, tail flick test, and hot plate test appeared normal (Supplementary Figure 2-4). These results suggest that YF/YF mice showed reduced susceptibility to depression, but other general behaviours, such as locomotor activity, cognitive function, anxiety-related behaviour, startle response, and pain behaviour are normal.

Increased Tyr 1325 phosphorylation by the forced swim test and the tail suspension test

We next investigated whether the level of Tyr 1325 phosphorylation in the striatum, one of the brain regions involved in depression (Petit-Demouliere *et al*, 2005), was affected by the forced swim test. At 5 min after the test, the mice were sacrificed, the striata were dissected out, and the lysates were prepared. The NR2A immunoprecipitates from these lysates were then subjected to immunoblotting with the anti-pY1325 antibody followed by re-blot with the anti-NR2A antibody. As shown in Figure 6A, the level of Tyr 1325 phosphorylation was increased significantly in the striatum in mice exposed to the forced swim test compared with control ($n=3$; $^*P<0.05$, Student's t test). Likewise, the level of Tyr 1325 phosphorylation was also increased in the striatum in mice exposed to the tail suspension test ($n=5$; $^*P<0.05$, Student's t test; Figure 6B). We also found that Src was activated by the forced swim test using anti-Src (pY418) antibody specific to the active form of Src (Figure 6A; $n=3$; $^*P<0.05$, Student's t test). Neither Ser 896 phosphorylation on NR1 (Figure 6A) nor Tyr 1472 phosphorylation on NR2B (Figure 6A and B) was affected by the same stimulation. In addition, the level of Tyr 1325 phosphorylation in the striatum was not at all affected by the elevated plus maze and the open field test (Supplementary Figure 5). These data suggest that Tyr 1325 phosphorylation of NR2A is relevant to the depression-related behaviour.

Normal monoamine systems in YF/YF mice

Given that depression-related behaviour is affected by monoamine systems (Cryan and Mombereau, 2004), we measured the amounts of monoamines and their metabolites in various

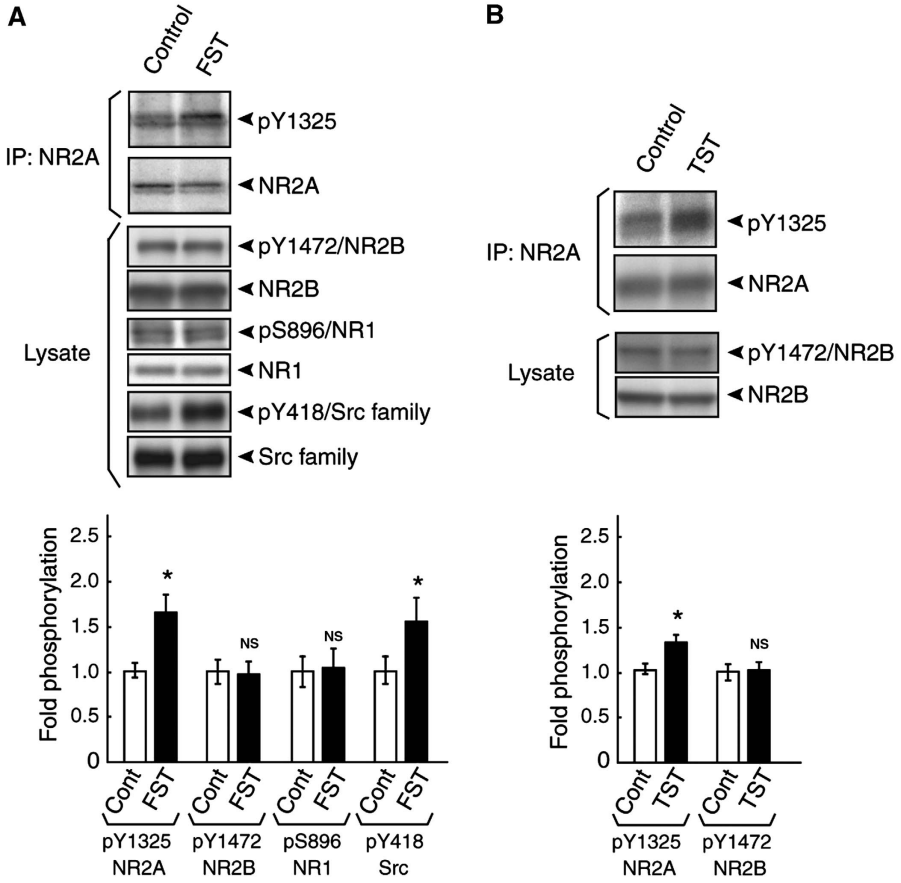

Figure 6 Increased Tyr 1325 phosphorylation during the forced swim test and the tail suspension test. (**A**) The level of Tyr 1325 phosphorylation in the striatum was increased during the forced swim test. Equal amounts of NR2A immunoprecipitates from lysates of the forced swim test-exposed mice and control mice were probed using the anti-Tyr 1325 antibody followed by a re-blot with the anti-NR2A antibody. $^*P<0.05$, $n=3$, Student's t-test. The levels of Tyr 1472 phosphorylation on NR2B and Ser 896 phosphorylation on NR1 were unchanged after the forced swim test. Equal amounts of striatal lysates from the forced swim test-exposed mice and control mice were subjected to immunoblotting with antibodies against pY1472/NR2B, NR2B, pS896/NR1, NR1, pY418/Src kinases, and Src kinases. ($P>0.05$, $n=3$, Student's t-test). It was noteworthy that Src was activated after the forced swim test. ($^*P<0.05$, $n=3$, Student's t test). FST, the forced swim test. (**B**) The level of Tyr 1325 phosphorylation in the striatum was increased during the tail suspension test. Equal amounts of NR2A immunoprecipitates from lysates of the tail suspension test-exposed mice and control mice were probed using the anti-Tyr 1325 antibody followed by re-blot using the anti-NR2A antibody. ($^*P<0.05$, $n=5$, Student's t-test). The level of Tyr 1472 phosphorylation on NR2B was unchanged by the tail suspension test. ($P>0.05$, $n=5$, Student's t-test). TST: the tail suspension test; NS: not significant.

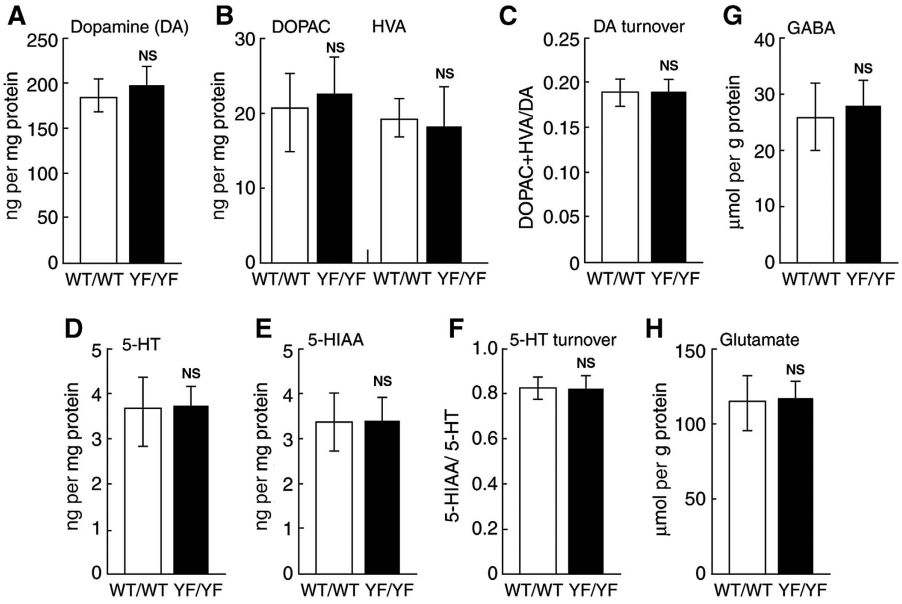

Figure 7 Normal amounts of monoamines, their metabolites, and amino acids in the striatum of YF/YF mice. (**A**–**F**) Biopsies of the striatum were obtained from frozen brain sections and monoamines and their metabolites were extracted and analysed. (A) The amount of dopamine (DA). (B) The amounts of DOPAC and HVA. (C) DA turnover. (D) The amount of serotonin (5-HT). (E) The amount of 5-HIAA. (F) 5-HT turnover. (**G**, **H**) Biopsies of the striatum were obtained from frozen brain sections and amino acids were derivatized with OPA and analysed. (G) The amount of GABA. (H) The amount of glutamate. No significant differences were observed between WT/WT and YF/YF mice for any of the measurements (WT/WT, $n=6$; YF/YF, $n=6$, $P>0.05$, one-way ANOVA). NS: not significant.

brain regions, including the hippocampus, hypothalamus, prefrontal cortex, and striatum of WT/WT and YF/YF mice (Figure 7A–F and data not shown). We did not detect any significant abnormalities in the levels of dopamine and serotonin and their metabolites in any of the brain region we examined, including the striatum of YF/YF mice (Figure 7A–F and data not shown), suggesting that monoamine systems are normal in YF/YF mice. In addition, the levels of glutamate and GABA were also unaltered in the striatum of YF/YF mice compared with those of WT/WT mice (Figure 7G and H).

Increased phosphorylation of DARPP-32 at Thr 34 in YF/YF mice

DARPP-32, a dopamine- and cAMP-regulated phosphoprotein of 32 kDa, is a signal transduction molecule that is highly enriched in medium spiny neurons of the neostriatum (Svenningsson *et al*, 2004). There is a report that DARPP-32 phosphorylation at Thr 34 is involved in the regulation of depression-related behaviours (Svenningsson *et al*, 2002). This led us to examine whether Thr 34 phosphorylation of DARPP-32 is altered in YF/YF mice. As shown in Figure 8A, Thr 34 phosphorylation of DARPP-32 was significantly increased in the striatum of YF/YF mice as compared with that of WT/WT mice (*$P<0.05$, Student's t test; Figure 8A). We then examined the ERK activity because Thr 34 phosphorylation of DARPP-32 occurs upstream of ERK activation (Valjent *et al*, 2005). We observed that the activity of ERK, evaluated by the anti-phospho-ERK specific antibody, was significantly higher in YF/YF mice compared with that in WT/WT mice (*$P<0.05$, Student's t test; Figure 8B). Therefore, we conclude that Thr 34 phosphorylation on DARPP-32 and the subsequent ERK activity are elevated in the absence of Tyr 1325 phosphorylation on the NR2A subunit. Given that Thr 34 phosphorylation of DARPP-32 is important for depression-related behaviour (Svenningsson *et al*, 2002, 2004), antidepressant-like phenotype of YF/YF mice may be attributable to increased Thr 34 phosphorylation of DARPP-32.

Decreased calcineurin activity in YF/YF mice

We next addressed the mechanism by which DARPP-32 phosphorylation at Thr 34 was increased in YF/YF mice. We focused on the Ca^{2+}/calmodulin-dependent protein phosphatase calcineurin, as it dephosphorylates Thr 34 of DARPP-32 downstream of NMDA receptor activation (Nishi *et al*, 2005). We analysed calcineurin activity in the striatum by measuring the free phosphate released from the synthetic RII phosphopeptide substrate, the most efficient and well-known peptide substrate of calcineurin (Enz *et al*, 1994). As expected, calcineurin activity was significantly decreased in YF/YF mice as compared with that in WT/WT mice (*$P<0.05$, Student's t test; Figure 8C). These results suggest that loss of Tyr 1325 phosphorylation downregulates calcineurin activity, and the impaired calcineurin activity is responsible for the increased DARPP-32 phosphorylation at Thr 34 (Figure 9). Intriguingly, however, we did not detect any significant reduction in CaMKII activity in YF/YF mice (Figure 8D), despite the fact that CaMKII activity is also regulated by Ca^{2+} (see Discussion).

Discussion

Accumulating evidence indicates that tyrosine phosphorylation of the NMDA receptor is an important step involved in the regulation of brain functions such as synaptic plasticity. The NR2A subunit of the NMDA receptor is abundantly tyrosine-phosphorylated by the Src family kinases (Tezuka *et al*, 1999), and Tyr 1292, Tyr 1325, and Tyr 1387 are reported

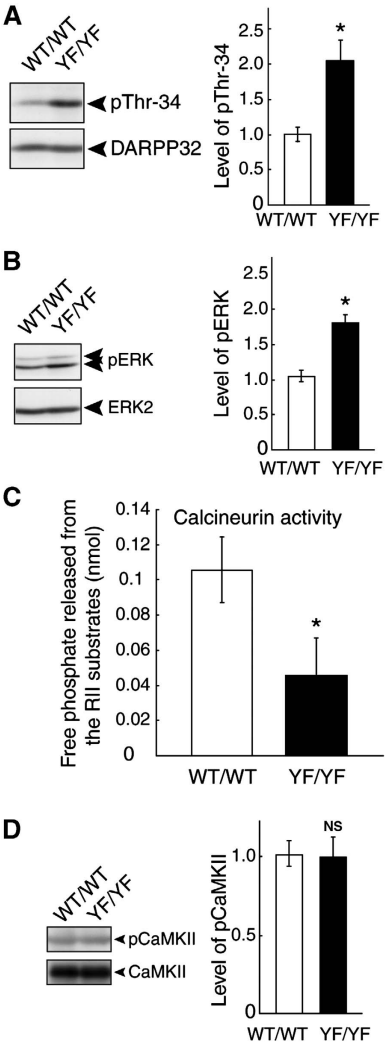

Figure 8 Increased DARPP-32 phosphorylation at Thr 34 and decreased calcineurin activity in YF/YF mice. (**A**) Increased DARPP-32 phosphorylation at Thr 34 in YF/YF mice. Striata from WT/WT and YF/YF mice were dissected and homogenized in TNE buffer. Then striatal lysates from WT/WT and YF/YF mice were subjected to immunoblotting with the anti-pThr 34 antibody, followed by a re-blot using the anti-DARPP-32 antibody. A representative blot is shown on the left ($^*P<0.05$, $n=3$, Student's *t*-test). (**B**) Increased ERK activity in YF/YF mice. Striatal lysates from WT/WT and YF/YF mice were subjected to immunoblotting with the anti-pERK (pT185 and pY187) antibody followed by re-blot with anti-ERK2 antibody. A representative blot is shown on the left ($^*P<0.05$, $n=3$, Student's *t*-test). (**C**) Decreased calcineurin activity in YF/YF mice. Calcineurin activity in the striatum from WT/WT and YF/YF mice was analysed by measuring free phosphate released from the synthetic RII phosphopeptide substrate as described in the Materials and methods ($^*P<0.05$, $n=3$, Student's *t*-test). (**D**) Normal CaMKII activity in YF/YF mice. Striatal lysates from WT/WT and YF/YF mice were subjected to immunoblotting with the anti-phospho-CaMKII (pT286) antibody followed by re-blot with anti-CaMKII antibody. A representative blot is shown on the left ($P>0.05$, $n=3$, Student's *t*-test). NS: not significant.

to be major phosphorylation sites in HEK 293T cells (Yang and Leonard, 2001). Here we have shown for the first time that Tyr 1325 is heavily phosphorylated not only in the cultured heterologous cells but also in the brain. In addition, we observed that Tyr 943, Tyr 1105, Tyr 1118, Tyr 1187, Tyr 1246, and Tyr 1267 could be phosphorylated by active Src (Figure 1 and data not shown). As we discuss below, we further provided evidence that Tyr 1325, that has been shown by us and others to be one of the major phosphorylation sites (Figure 1, Yang and Leonard, 2001), is critically involved in the regulation of NMDA receptor channel activity and in depression-related behaviour.

Our finding that mice carrying a mutation at Tyr 1325 phosphorylation site (YF/YF mice) showed reduced depression-related behaviour (Figure 5A and B) is consistent with previous studies showing antidepressant-like effects of NMDA receptor antagonists and reduced depression-related behaviour in NR2A null knockout mice (Boyce-Rustay and Holmes, 2006). Although NR2A null knockout mice show greatly increased locomotor activity in the open field test, which can confound the performance of the mouse in the forced swim test and in the tail suspension test (Miyamoto *et al*, 2001), YF/YF mice showed normal locomotor activity in the open field test (Figure 5C). Moreover, in contrast to NR2A null knockout mice, YF/YF mice showed normal cognitive functions and anxiety-like behaviours in various tests we performed (Figure 5 and Supplementary Figure 2–4). These results suggest that suppression of NR2A expression causes more general abnormalities in broader ranges of brain function than Y1325F mutation that produces specific abnormalities in depression-related behaviour. Consistent with this theory, we did not detect any significant abnormalities in the induction of long-term potentiation in the CA1 region of the hippocampus and in the NMDA receptor-mediated signalling in the prefrontal cortex (Supplementary Figure 6 and 7). The increase in Tyr 1325 phosphorylation in the striatum on exposure of mice to the forced swim test and the tail suspension test further supports the idea that Tyr 1325 phosphorylation is relevant for depression-related behaviour (Figure 6). In addition, we did not detect significant increases in the level of tyrosine phosphorylation of the Y1325F-containing NR2A subunit after the forced swim test (Supplementary Figure 8), suggesting that phosphorylation sites other than Tyr 1325 in the NR2A subunit is not relevant for the depression-related behaviour.

In YF/YF mice, the amounts of monoamines, their metabolites, and GABA levels were observed to be normal (Figure 7). Furthermore, PKA activity that is regulated by dopamine receptors was normal in the striatum of YF/YF mice (Supplementary Figure 9). These results suggest that the monoamine systems and the GABA system that were shown to be involved in depression-related behaviour (Cryan and Mombereau, 2004) were normal in YF/YF mice. Although the possibility that other neurochemical changes underlie the behavioural abnormalities observed here cannot be ruled out, we would like to emphasize that NMDA receptor-mediated signalling is selectively impaired in YF/YF mice. Given that NMDA receptor-mediated Thr 34 phosphorylation of DARPP-32 is important for depression-related behaviour (Svenningsson *et al*, 2002, 2004; Nishi *et al*, 2005), the antidepressant-like phenotype of YF/YF mice may be attributable partly to increased Thr 34 phosphorylation of DARPP-32. Although glutamatergic signalling regulates DARPP-32 phosphorylation (Nishi *et al*, 2005), it is unclear how the activity of NMDA receptor is involved in the DARPP-32 phosphorylation *in vivo*. Our result provides the first genetic evidence for the involvement of tyrosine phosphorylation of NMDA receptor in DARPP-32 phosphorylation.

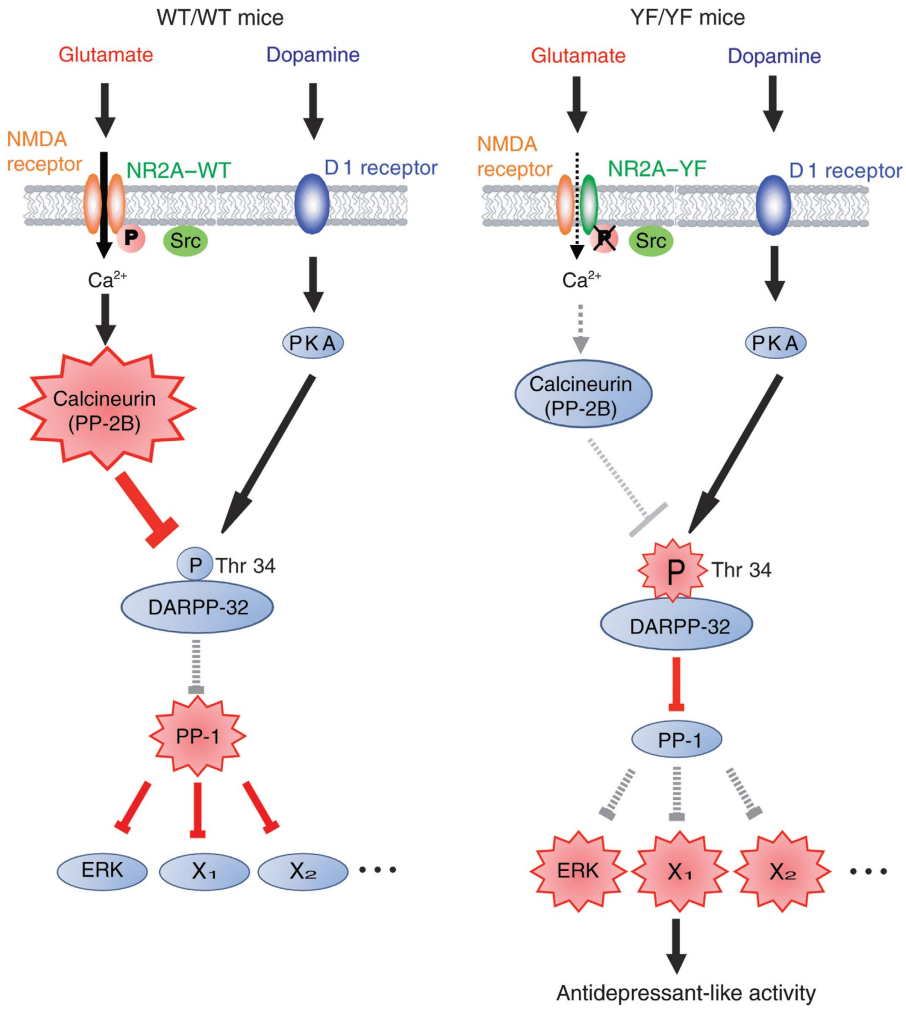

Figure 9 A proposed model for the role of Tyr 1325 phosphorylation on NR2A subunit in depression-related behaviour. (left) In WT/WT mice, Src-mediated Tyr 1325 phosphorylation increases the Ca^{2+} influx through the NR2A subunit-containing NMDA receptor channels, and thereby activates a Ca^{2+}-dependent protein phosphatase, calcineurin. Activated calcineurin then de-phosphorylates Thr 34 of DARPP-32, leading to the generation of active protein phosphatase-1 (PP-1). Consequently, the phosphorylation levels of PP-1 substrates, including ERK, are decreased. (right) In YF/YF mice, Ca^{2+} influx through the NR2A subunit-containing NMDA receptor channels is decreased in the absence of Tyr 1325 phosphorylation, resulting in decreased calcineurin activity and increased phosphorylation of Thr 34 on DARPP-32. Phosphorylation of Thr 34 on DARPP-32 converts DARPP-32 into a potent inhibitor of PP-1, and thereby increases the phosphorylation level of PP-1 substrates including ERK. The antidepressant-like phenotype of YF/YF mice may be attributable partly to the increased Thr 34 phosphorylation of PP-1 substrates including ERK.

The mechanism by which Src-family kinases are activated is unknown. As stimulation of metabotropic glutamate receptors (mGluRs) activates Src to regulate NMDA receptors in cortical neurons (Heidinger *et al*, 2002), it is possible that mGluR activation increases Src-mediated Tyr 1325 phosphorylation. Interestingly, mGluR antagonists have antidepressant-like effects in the forced swim test and the tail suspension test (Belozertseva *et al*, 2007), suggesting that Tyr 1325 phosphorylation on the NR2A subunit may be relevant to mGluR-mediated regulation of depression-related behaviour.

We observed that Src-induced potentiation of NMDA receptor-mediated currents and increase in Ca^{2+} levels were abolished in NR1/NR2A–Y1325F channels (Figures 2 and 4). Furthermore, we found that calcineurin activity was downregulated in the striatum of YF/YF mice (Figure 8), which is responsible for the decrease in DARPP-32 phosphorylation at Thr 34 (Nishi *et al*, 2005). Thus, our current results argue that the Ca^{2+} influx through the NR2A subunit-containing NMDA receptor channels is decreased in the absence of Tyr 1325 phosphorylation, resulting in decreased calcineurin activity and increased phosphorylation of one of the calcineurin substrates, DARPP-32 (see Figure 9). In YF/YF mice, we did not detect a significant reduction in CaMKII activity (Figure 8D) that is also regulated by Ca^{2+} influx through NMDA receptors. Previous studies have established that calcineurin is much more sensitive to the increase in Ca^{2+} concentrations in the post-synaptic cell than CaMKII (Xia and Storm, 2005; Irvine *et al*, 2006), suggesting that the lack of change in CaMKII activity may be explained by the difference in the sensitivity between CaMKII and calcineurin towards Ca^{2+}. Src family kinase-mediated Tyr 1325 phosphorylation of the NR2A subunit would induce relatively low and sustained increase in NMDA receptor-mediated

currents, which is sufficient to activate calcineurin. In contrast, larger increase in NMDA receptor-mediated currents may be required to affect CaMKII activity.

Previous studies illustrate that endogenous Src activity enhances NMDA receptor-mediated currents by facilitating NMDA receptor channel gating without affecting the NMDA receptor single-channel conductance (Wang and Salter, 1994; Yu *et al*, 1997). Our data suggest that Tyr 1325 phosphorylation is responsible for Src-induced facilitation of NMDA receptor channel gating (Figures 2 and 4). Though the mechanism behind it is not clear, Tyr 1325 phosphorylation may lead to conformational change of the NMDA receptor channel that increases ionic flux. Alternatively, Tyr 1325 phosphorylation may regulate the interaction between the NMDA receptor and an unidentified protein that regulates the NMDA receptor channel property. Intriguingly, a previous report has shown that Tyr 1105, Tyr 1267, and Tyr 1387 sites are also important for Src-mediated potentiation of NMDA receptor-mediated currents in HEK293T cells (Zheng *et al*, 1998). Although our electrophysiological studies reveal complete abolishment of Src-induced potentiation of NMDA-mediated receptor current in NR1/NR2A–Y1325F channels (Figure 2), Tyr 1325 phosphorylation, together with the phosphorylation on the other sites, may cooperatively regulate NMDA receptor-mediated currents. The mechanism behind the possible cooperative action needs to be addressed in future studies.

In summary, this study demonstrates that NR2A tyrosine phosphorylation at Tyr 1325 is important for depression-related behaviour in the tail suspension test and the forced swim test. The emotion-related phenotype of YF/YF mice was not probably due to the deficits in general physical activity or gross abnormalities in brain development and neurological functions. Therefore, YF/YF mice would serve as a useful animal model to study the pathogenesis of mood disorders and to develop therapeutic drugs for the disease.

Materials and methods

Purification of GST fusion proteins

Fusion proteins, GST–C1, GST–C2, GST–C3, and GST–C2–Y1325F were expressed in *Escherichia coli* BL21. Purification of GST fusion proteins was performed as described previously by Nakazawa *et al* (2001).

Tryptic peptide mapping analysis

Tryptic peptide mapping of GST fusion proteins was performed as described previously by Nakazawa *et al* (2001).

Cell culture and transient transfection

The culture of HEK 293T cells and their transient transfection were performed as described previously by Nakazawa *et al* (2001).

Preparation of lysate, immunoprecipitation and immunoblotting

Preparation of lysate from the mouse brain, immunoprecipitation, and immunoblotting were performed as described previously by Nakazawa *et al* (2006). For quantification, the immunoreacted protein bands were analysed using the NIH image software.

Antibodies

Rabbit polyclonal antibodies against phospho-Tyr 1325 were raised using a keyhole limpet hemocyanin-conjugated synthetic phosphopeptide around Tyr 1325 as immunogen. The antibody was purified from sera of the immunized rabbits by successive affinity chromatography. The anti-NR2A antibody and anti-pY1472/NR2B antibodies have been described in previous studies (Tezuka *et al*, 1999; Nakazawa *et al*, 2001). Commercially available antibodies used in this study are: anti-phosphotyrosine (4G10; Upstate Biotechnology, Waltham, MA, USA); anti-phospho Thr 34 DARPP-32 (PhosphoSolutions, Aurora, CO, USA); anti-DARPP-32 (PhosphoSolutions); anti-phospho ERK (Cell Signaling Technology, Beverly, MA, USA); anti-ERK2 (Santa Cruz Biotechnology, Santa Cruz, CA, USA); anti-phospho-Src (Cell Signaling Technology); anti-Src family (Santa Cruz Biotechnology); anti-phospho-CaMKII (pT286; Promega, Madison, WI, USA); and anti-CaMKII (Chemicon International, Temecula, CA, USA) antibodies.

Electrophysiology in HEK293T cells

Cloned cDNAs for the rat NMDA receptor subunits NR1E and NR2A, inserted into the eukaryotic expression vector pME, were used to transfect HEK 293T cells as described by Nakazawa *et al* (2001). Whole-cell recordings were performed as described previously by Miwa *et al* (2008). Cells on coverslips were kept in a chamber continuously perfused with Ringer's solution (135 mM NaCl, 5.4 mM KCl, 1.8 mM $CaCl_2$, 5 mM HEPES (pH 7.2), 10 mM glucose), which was saturated with 95% O_2 and 5% CO_2. During giga-seal formation, single captured cells were lifted from the bottom of the dishes. After establishing the whole-cell configuration, short pulses of NMDA stimulus solution (100 μM NMDA and 10 μM glycine in Ringer's solution: 0.5 s) were applied to the recorded cell every 30 s with the local perfusion system (SF-77B Perfusion Fast-Step, Harvard Apparatus, Hamden, CT, USA). The patch pipette solution contained: 140 mM CsCl, 1.0 mM $MgCl_2$, 0.1 mM EGTA, 10 mM HEPES (pH 7.2), 4 mM ATP with or without recombinant Src (30 U/ml) (Upstate Biotechnology). The NMDA receptor-mediated currents were recorded at a holding potential of −60 mV. MultiClamp 700A amplifier and Digidata 1322A (Molecular Devices, Sunnyvale, CA, USA) were used to record and store data using the pClamp software (Molecular Devices), respectively. All experiments were performed at 25–28°C.

Calcium measurements

Measurements of cytosolic free calcium concentrations using an acetoxymethyl ester of fura-2 (fura-2/AM; Invitrogen, Carlsbad, CA, USA) were performed as described previously by Yokoyama *et al* (2002). The ratio of increase in Ca^{2+} concentration, during the 30-s interval after NMDA stimulation (500 μM) relative to that during the 30-s interval before the NMDA stimulation in cells expressing NR1/WT–NR2A (without Src), was assigned the arbitrary value 1.

Generation of YF/YF mice

To construct the targeting vector, a genomic DNA fragment carrying the carboxy-terminal coding region of the *NR2A* gene was isolated from a C57BL/6 genomic library (Stratagene, La Jolla, CA, USA). The 3′ fragment of *NR2A* contained the Tyr 1325 mutated to phenylalanine. Embryonic stem cell line E14.1 (129/Ola-derived) was electroporated with the linearized targeting vector, and positive clones were identified by PCR and confirmed by Southern blotting using the outer probe. Positive clones were used to generate chimeric mice through the aggregation method. The chimeric mice were crossed to the transgenic mice carrying the CAG–cre transgene with C57BL/6 background (Sakai and Miyazaki, 1997) to remove the neo cassette through *Cre/lox-P*-mediated excision. After confirmation of the loss of the *neo* gene by PCR and Southern blotting, the mice were crossed to C57BL/6J mice to yield heteromeric F2 mice with a 75% pure C57BL/6J genetic background. Heterozygous mice were backcrossed successively to C57BL/6J mice to yield subsequent generations with more pure C57BL/6J genetic backgrounds. F5–7 heterozygous mice were crossed to each other to yield homozygous mice and wild-type littermates. Experiments using animals were carried out in accordance with the guidelines for animal use issued by the Committee of Animal Experiments, Institute of Medical Science, University of Tokyo.

Histology

Histological analyses were performed as described previously by Nakazawa *et al* (2006).

Electrophysiology in medium spiny neurons lin acute striatal slices

Coronal brain slices containing the cortex and the striatum (300 μm thick) were prepared from WT/WT or YF/YF mice at postnatal day

16–28 as described previously by Narushima *et al* (2006). In brief, mice were decapitated under anaesthesia with 100% CO_2, and the brains were cooled in ice-cold, modified external solution(120 mM Choline–Cl, 2 mM KCl, 8 mM $MgCl_2$, 28 mM $NaHCO_3$, 1.25 mM $NaHPO_4$, and 20 mM glucose (bubbling with 95% O_2 and 5% CO_2)). Slices were cut using a Leica VT1200 slicer (Wetzlar, Germany). For recovery, slices were incubated for at least 1 h in the normal bathing solution(125 mM NaCl, 2.5 mM KCl, 2 mM $CaCl_2$, 1 mM $MgSO_4$, 1.25 mM NaH_2PO_4, 26 mM $NaHCO_3$, and 20 mM glucose (pH 7.4) (bubbling with 95% O_2 and 5% CO_2)).

Whole-cell recordings were made from medium spiny neurons in the dorsolateral region of the striatum using an upright microscope (BX50WI; Olympus Optical, Tokyo, Japan) equipped with an infrared CCD camera system (Hamamatsu Photonics, Hamamatsu, Japan). Medium spiny neurons were identified visually through their medium-sized, spherical somata as well as their electrophysiological properties (Kita *et al*, 1984). Resistance of the patch pipette was 2–3 MΩ when filled with the intracellular solution 60 mM CsCl, 10 mM Cs-gluconate, 20 mM TEA–Cl, 30 mM HEPES, 20 mM BAPTA-K_4, 4 mM $MgCl_2$, 4 mM Na_2-ATP, 0.4 mM Na_2-GTP (pH 7.3, adjusted with CsOH). Membrane currents were recorded with an EPC9/2 amplifier (HEKA Electronik, Lambrecht/Pfalz, Germany) and the pipette access resistance was compensated by 80%. The PULSE software (HEKA Electronik) was used for stimulation and data acquisition. The signals were filtered at 3 kHz and digitized at 20 kHz. To stimulate corticostriatal axons, two glass micropipettes filled with the normal saline were placed in the cerebral cortex or in the underlying white matter. Stimulus pulses (duration: 0.1 ms; intensity: 0–80 V) were applied between the pipettes to evoke EPSCs in medium spiny neurons.

For assessing the effect of Src on NMDA receptor-mediated EPSCs, Src (60 U/ml) was applied intracellularly from the recording pipette by diffusion. At the holding potential of +50 mV, NMDA receptor-mediated EPSCs were monitored after every 20 s starting from 2 min after the establishment of whole-cell recording. The bath solution was supplemented with picrotoxin (100 μM) and NBQX (10 μM) to block $GABA_A$ receptor-mediated inhibitory post-synaptic currents and AMPA receptor-mediated EPSCs, respectively.

Tail suspension test

Mice (8–10-week-old) were suspended above the floor by fixing the end of their tail to wire netting. The mice were manually observed for the presence or absence of immobility during the 6-min test session. All behavioural experiments were performed blindly.

Forced swim test

Mice (8–10-week-old) were placed in a cylinder filled with water temperature of which was between 23 and 25°C. The mice were manually observed for the presence or absence of immobility during the 10-min test session.

Open field test

The apparatus was a square arena (50 × 50 × 33.3 cm (W × D × H)) made of polyvinyl chloride. A mouse was placed in the perimeter and allowed to explore the apparatus for 15 min. The total distance travelled in the arena, the time spent in the centre (30 × 30 cm), and rearing activity were analysed with a Macintosh computer using Image OFCR 1.00× and Image OF circle 1.01× (O'Hara & Co. Ltd., Tokyo, Japan), a modified software based on the public domain of NIH Image programme.

Light–dark emergence test

The light–dark box consisted of two compartments: a transparent polyvinyl chloride box (100 lux) and a black polyvinylchloride box (both 19 × 19 × 19 cm). Two boxes were separated by a vertical sliding door that remained open (5 × 5 cm). The amount of time spent in the transparent and black boxes was measured for 10 min.

Social interaction test

A male subject mouse was placed in a neutral cage for 30 min, after which a juvenile (5 weeks of age) conspecific male subject was introduced. The interaction between the male subject and the juvenile conspecific male subject was recorded using a video camera for 3 min. Social interaction was determined as the total amount of time that the male subject spent on interaction with the juvenile conspecific male subject.

Elevated plus maze test

The elevated plus maze (EP-3002; O′ Hara & Co. Ltd.) consisted of two open arms (25 × 5 cm) and two enclosed arms of the same size extending from a central area (5 × 5 cm) and elevated 50 cm from the ground. Mice were placed in the central square of the maze facing one of the open arms. Mouse behaviour was recorded during a 10-min test period by means of a Macintosh computer using Image OFCR 1.00× and Image OF circle 1.01× (O'Hara & Co. Ltd.), a modified software based on the public domain of NIH Image programme. The following conventional parameters were recorded: the number of entries into open or closed arms and the time spent in open or closed arms. The number of head dips (a behaviour in which the mouse dips its head into open space and observes the environment while the body is in an open arm) was also recorded.

Measurement of monoamines and amino acids

Circular tissue punches (1 mm diameter) were taken from 150-μm thick frozen coronal brain sections obtained from 8-week-old mice ($n = 6$ per group) and stored at −80°C until assayed. Monoamines, amino acids, and metabolites were extracted by sonication in 0.1 M perchloric acid containing a mixture of internal standards (200 nM isoproterenol, 200 μM L-norleucine, and 5 μM ethylhomocholine). Protein contents were measured using a DC Protein Assay Kit (Bio-Rad, Hercules, CA, USA). The remainder of the sample was centrifuged for 15 min at 15 000 r.p.m. and the supernatant filtered through 0.22-mm micropore, polyvinylidene fluoride filters (Millipore Corp. Billerica, MA, USA) by centrifugation (14 000 r.p.m. for 5 min). The filtrate was analysed by high-pressure liquid chromatography coupled to electrochemical detection (Eicom, Kyoto, Japan). Briefly, an Eicompak SC-5ODS 3.0 × 150 mm column was used for separations, perfused with a mobile phase consisting of citrate (41.4 mM), sodium acetate (39.2 mM), methanol (17%), sodium 1-octanesulfonate (190 mg/l), and EDTA (5 mg/l), adjusted to pH 3.7 using glacial acetic acid and pumped at a rate of 0.5 ml/min. The working electrode (WE-3G) potential was set at +0.75 V. Amino acid content was analysed by HPLC using fluorometric detection. Amino acids were derivatized with o-phthalaldehyde (OPA) before automated injection into the HPLC column (methods essentially similar to Murphy and Maidment (1999)) and resolved using a gradient on a reverse-phase column with sodium acetate (35 mM, pH 5.9 adjusted using glacial acetic acid), 1% tetrahydrofuran, as aqueous solvent. The organic mobile phase consisted of 70% acetonitrile, 15% methanol, and 35 mM sodium acetate (pH 7.65, adjusted using glacial acetic acid). The flow rate was 0.6 ml/min. Data were collected and analysed by Ezchrom Elite software (Scientific Software, Lincolnwood, IL, USA). All analysis information, including the retention times, peak heights, concentrations, and recovery rate of internal standards, were calculated by comparison to standard curves generated for known concentrations of external standards that were run daily. Turnover rates were calculated as follows: dopamine (DA) turnover rate = [3,4-dihydroxyphenylacetic acid (DOPAC)] + [homovanillic acid (HVA)]/[DA]; serotonin (5-HT) turnover rate = [5-hydroxyindoleacetic acid (5-HIAA)]/[5-HT].

Measurement of calcineurin activity

Calcineurin activity was measured by using the synthetic phosphorylated RII peptide using a calcineurin assay kit (Biomol, Plymouth Meeting, PA, USA) following the manufacturer's instructions.

Statistical analysis

All data are expressed as mean ± s.e.m values. Statistical analysis was done using Student's *t*-test, paired *t*-test, and one-way ANOVA. Differences with $P < 0.05$ were considered as significant.

Supplementary data

Supplementary data are available at *The EMBO Journal* Online (http://www.embojournal.org).

Acknowledgements

We thank J. Miyazaki for providing the mice carrying the CAG–cre transgene and S. Nakanishi for providing cDNAs of the rats NR1E and NR2A. We thank S. Kida for helpful discussion. We also thank the editorial assistance of the NIH Fellows Editorial Board. This

research was supported in part by Grants-in-Aid for Scientific Research (TN, TY, AMW, and TM); by Global COE Program (Integrative Life Science Based on the Study of Biosignaling Mechanisms) (TY); by Center for Brain Medical Science, 21st Century COE Program (TM); and by Global COE Program (Comprehensive Center of Education and Research for Chemical Biology of the Diseases) (TM) from the Ministry of Education, Science, Sports, Culture and Technology of Japan.

Conflict of interest

The authors declare that they have no conflict of interest.

References

Belozertseva IV, Kos T, Popik P, Danysz W, Bespalov AY (2007) Antidepressant-like effects of mGluR1 and mGluR5 antagonists in the rat forced swim and the mouse tail suspension tests. *Eur Neuropsychopharmacol* **17:** 172–179

Boyce-Rustay JM, Holmes A (2006) Genetic inactivation of the NMDA receptor NR2A subunit has anxiolytic- and antidepressant-like effects in mice. *Neuropsychopharmacology* **31:** 2405–2414

Chen BS, Roche KW (2007) Regulation of NMDA receptors by phosphorylation. *Neuropharmacology* **53:** 362–368

Choi DW (1988) Calcium-mediated neurotoxicity: relationship to specific channel types and role in ischemic damage. *Trend Neurosci* **11:** 465–469

Collingridge GL, Bliss TVP (1995) Memories of NMDA receptors and LTP. *Trend Neurosci* **18:** 54–56

Cryan JF, Mombereau C (2004) In search of a depressed mouse: utility of models for studying depression-related behavior in genetically modified mice. *Mol Psychiatry* **9:** 326–357

Cryan JF, Mombereau C, Vassout A (2005) The tail suspension test as a model for assessing antidepressant activity: review of pharmacological and genetic studies in mice. *Neurosci Biobehav Rev* **29:** 571–625

Crawley JN (2007) in *What's wrong with my mice? Behavioral phenotyping of transgenic and knockout mice*, 2nd edition. Wiley-Liss: New York

Cull-Candy S, Brickley S, Farrant M (2001) NMDA receptor subunits: diversity, development and disease. *Curr Opin Neurobiol* **11:** 327–335

Enz A, Shapiro G, Chappuis A, Dattler A (1994) Nonradioactive assay for protein phosphatase 2B (calcineurin) activity using a partial sequence of the subunit of cAMP-dependent kinase as substrate. *Anal Biochem* **216:** 147–153

Heidinger V, Manzerra P, Wang XQ, Strasser U, Yu SP, Choi DW, Behrens MM (2002) Metabotropic glutamate receptor 1-induced upregulation of NMDA receptor current: mediation through the Pyk2/Src-family kinase pathway in cortical neurons. *J Neurosci* **22:** 5452–5461

Husi H, Ward MA, Choudhary JS, Blackstock WP, Grant SG (2000) Proteomic analysis of NMDA receptor-adhesion protein signaling complex. *Nat Neurosci* **3:** 661–669

Irvine EE, von Hertzen LS, Plattner F, Giese KP (2006) alphaCaMKII autophosphorylation: a fast track to memory. *Trends Neurosci* **29:** 459–465

Ishii T, Moriyoshi K, Sugihara H, Sakurada K, Kadotani H, Yokoi M, Akazawa C, Shigemoto R, Mizuno M, Masu M (1993) Molecular characterization of the family of the *N*-methyl-D-aspartate receptor subunits. *J Biol Chem* **268:** 2836–2843

Kita T, Kita H, Kitai ST (1984) Passive electrical membrane properties of rat neostriatal neurons in an *in vitro* slice preparation. *Brain Res* **300:** 129–139

Kohr G, Seeburg PH (1996) Subtype-specific regulation of recombinant NMDA receptor-channels by protein tyrosine kinases of the src family. *J Physiol* **492:** 445–452

Kornau HC, Seeburg PH, Kennedy MB (1997) Interaction of ion channels and receptors with PDZ domain proteins. *Curr Opin Neurobiol* **7:** 368–373

Kutsuwada T, Kashiwabuchi N, Mori H, Sakimura K, Kushiya E, Araki K, Meguro H, Masaki H, Kumanishi T, Arakawa M, Mishina M (1992) Molecular diversity of the NMDA receptor channel. *Nature* **358:** 36–41

McDonald JW, Johnston MV (1990) Physiological and pathophysiological roles of excitatory amino acids during central nervous system development. *Brain Res Rev* **15:** 41–70

Miwa H, Fukaya M, Watabe AM, Watanabe M, Manabe T (2008) Functional contributions of synaptically localized NR2B subunits of the NMDA receptor to synaptic transmission and long-term potentiation in the adult mouse CNS. *J Physiol* **586:** 2539–2550

Miyamoto Y, Yamada K, Noda Y, Mori H, Mishina M, Nabeshima T (2001) Hyperfunction of dopaminergic and serotonergic neuronal systems in mice lacking the NMDA receptor ε1 subunit. *J Neurosci* **21:** 750–757

Mohn AR, Gainetdinov RR, Caron MG, Koller BH (1999) Mice with reduced NMDA receptor expression display behaviors related to schizophrenia. *Cell* **98:** 427–436

Monyer H, Sprengel R, Schoepfer R, Herb A, Higuchi M, Lomeli H, Burnashev N, Sakmann B, Seeburg PH (1992) Heteromeric NMDA receptors: molecular and functional distinction of subtypes. *Science* **256:** 1217–1221

Murphy NP, Maidment NT (1999) Orphanin FQ/nociceptin modulation of mesolimbic dopamine transmission determined by microdialysis. *J Neurochem* **73:** 179–186

Nakazawa T, Komai S, Tezuka T, Hisatsune C, Umemori H, Semba K, Mishina M, Manabe T, Yamamoto T (2001) Characterization of Fyn-mediated tyrosine phosphorylation sites on GluRε2 (NR2B) subunit of the *N*-methyl-D-aspartate receptor. *J Biol Chem* **276:** 693–699

Nakazawa T, Komai S, Watabe AM, Kiyama Y, Fukaya M, Arima-Yoshida F, Horai R, Sudo K, Ebine K, Delawary M, Goto J, Umemori H, Tezuka T, Iwakura Y, Watanabe M, Yamamoto T, Manabe T (2006) NR2B tyrosine phosphorylation modulates fear learning as well as amygdaloid synaptic plasticity. *EMBO J* **25:** 2867–2877

Narushima M, Hashimoto K, Kano M (2006) Endocannabinoid-mediated short-term suppression of excitatory synaptic transmission to medium spiny neurons in the striatum. *Neurosci Res* **54:** 159–164

Nishi A, Watanabe Y, Higashi H, Tanaka M, Nairn AC, Greengard P (2005) Glutamate regulation of DARPP-32 phosphorylation in neostriatal neurons involves activation of multiple signaling cascades. *Proc Natl Acad Sci USA* **102:** 1199–1204

Okabe S (2007) Molecular anatomy of the postsynaptic density. *Mol Cell Neurosci* **34:** 503–518

Orrego F, Villanueva S (1993) The chemical nature of the main central excitatory transmitter: a critical appraisal based upon release studies and synaptic vesicle localization. *Neuroscience* **56:** 539–555

Petit-Demouliere B, Chenu F, Bourin M (2005) Forced swimming test in mice: a review of antidepressant activity. *Psychopharmacology* **177:** 245–255

Salter MW, Kalia LV (2004) Src kinases: a hub for NMDA receptor regulation. *Nat Rev Neurosci* **5:** 317–328

Sanacora G, Zarate CA, Krystal JH, Manji HK (2008) Targeting the glutamatergic system to develop novel, improved therapeutics for mood disorders. *Nat Rev Drug Disc* **7:** 426–437

Sakai K, Miyazaki J (1997) A transgenic mouse line that retains Cre recombinase activity in mature oocytes irrespective of the cre transgene transmission. *Biochem Biophys Res Commun* **237:** 318–324

Scannevin RH, Huganir RL (2000) Postsynaptic organization and regulation of excitatory synapses. *Nat Rev Neurosci* **1:** 133–141

Sheng M, Kim MJ (2002) Postsynaptic signaling and plasticity mechanisms. *Science* **298:** 776–780

Svenningsson P, Nishi A, Fisone G, Girault JA, Nairn AC, Greengard P (2004) DARPP-32: an integrator of neurotransmission. *Annu Rev Pharmacol Toxicol* **44:** 269–296

Svenningsson P, Tzavara ET, Witkin JM, Fienberg AA, Nomikos GG, Greengard P (2002) Involvement of striatal and extrastriatal DARPP-32 in biochemical and behavioral effects of fluoxetine (Prozac). *Proc Natl Acad Sci USA* **99:** 3182–3187

Tezuka T, Umemori H, Akiyama T, Nakanishi S, Yamamoto T (1999) PSD-95 promotes Fyn-mediated tyrosine phosphorylation of the *N*-methyl-D-aspartate receptor subunit NR2A. *Proc Natl Acad Sci USA* **96:** 435–440

Trullas R, Skolnick P (1990) Functional antagonists at the NMDA receptor complex exhibit antidepressant actions. *Eur J Pharmacol* **185:** 1–10

Valjent E, Pascoli V, Svenningsson P, Paul S, Enslen H, Corvol JC, Stipanovich A, Caboche J, Lombroso PJ, Nairn AC, Greengard P (2005) Regulation of a protein phosphatase cascade allows convergent dopamine and glutamate signals to activate ERK in the striatum. *Proc Natl Acad Sci USA* **102:** 491–496

Wang YT, Salter MW (1994) Regulation of NMDA receptors by tyrosine kinases and phosphatases. *Nature* **369:** 233–235

Xia Z, Storm DR (2005) The role of calmodulin as a signal integrator for synaptic plasticity. *Nat Rev Neurosci* **6:** 267–276

Yang M, Leonard JP (2001) Identification of mouse NMDA receptor subunit NR2A C-terminal tyrosine sites phosphorylated by coexpression with v-Src. *J Neurochem* **77:** 580–588

Yokoyama K, Su I-h, Tezuka T, Yasuda T, Mikoshiba K, Tarakhovsky A, Yamamoto T (2002) BANK regulates BCR-induced calcium mobilization by promoting tyrosine phosphorylation of IP_3 receptor. *EMBO J* **21:** 83–92

Yu XM, Askalan R, Keil GJ, Salter MW (1997) NMDA receptor channel regulation by channel-associated protein tyrosine kinase Src. *Science* **275:** 674–678

Zarate Jr CA, Singh J, Manji HK (2006) Cellular plasticity cascades: targets for the development of novel therapeutics for bipolar disorder. *Biol Psychiatry* **59:** 1006–1020

Zheng F, Gingrich MB, Traynelis SF, Conn PJ (1998) Tyrosine kinase potentiates NMDA receptor currents by reducing tonic zinc inhibition. *Nat Neurosci* **1:** 185–191